STABILITY OF SATURATED SAND DURING EARTHQUAKE

BY ZDENEK BAZANT*

ABSTRACT

There are many examples of liquefaction and of great subsidence in earthquake areas underlain by saturated sand. Therefore it is of interest to know how the stability of sand is affected by the earthquake. This case is studied as the state of stress in dynamically excited soil by the use of Mohr's diagram (Fig.1). The acceleration of an earthquake creates either dynamic stability of sand, compaction or liquefaction. As criteria differentiating these states are serving the critical acceleration (Fig.2) and the liquefactional acceleration (Fig.3), which upon the result of dimensional analysis are the function of five variables given by Eq. (15). From this equation it is possible to predict the behaviour of saturated sand during earthquake for a given dry density, height and volume of sand layer. Equation (15) is to be solved experimentally (Fig. 2 and 3).

NOTATIONS

f frequency

f_n natural frequency

g acceleration of gravity

t time

u_d dynamic pore pressure

u_s static pore pressure

v_p velocity of push wave

w vertical displacement

z vertical distance (depth)

A amplitude

D Mohr's envelope for dynamic case

H height of sand layer

S Mohr's envelope for static case

T resistance of water

* Professor of Foundation Engineering, Technical University, Prague, Czechslovakia.

V volume of sand layer

α acceleration of vibration (maximal)

α_c critical acceleration (maximal)

α_ℓ liquefactional acceleration (maximal)

γ_d dry density

γ_{dv} vibration density

γ_s unit weight of grains

γ_w unit weight of water

γ' unit weight of submerged soil

σ_d dynamic normal stress

σ_p expansion pressure

σ_s static normal stress

σ'_d dynamic effective stress

σ'_s static effective stress

τ shear stress

ϕ angle of internal friction

ϕ_v external variable force

BEHAVIOUR OF SATURATED SAND DURING EARTHQUAKES

Damage to buildings and bridges founded on saturated sand is known to be greater than on dry sand or rock. This is due to compaction or liquefaction of saturated sand caused by the acceleration of the earthquake, resulting in the subsidence of building structures.

A typical example of liquefaction was the New Madrid earthquake, Missouri U.S.A., of 1811 and 1812, located in the flood plain of the Mississippi River (Fuller 1912). Devastation rendered the area temporarily uninhabitable. Evidence of damage was still clearly visible when investigated one hundred years later and affected an area of 3690 sq. km. Devastation was caused by liquefaction of sand strata covered partly by recent silt and clay deposits. Liquefaction of sand created subsidence of the surface from 30 to 60 cm., springs and crevasses in surface layer with outflow of sand and streams of sand on the surface. The sand deposition

during earthquake on the surface occurred in the form locally known as sand boils (cones of sand), sand sloughs (sand in linear depressions) and sand scatters (thin surface coverings of sand). No sand was transported to the surface in the area of sunk lands, which are in the author's opinion the result of subsidence of liquefied sand compacted by earthquake. Springs and cones, known as sand boils, are locally observed in the New Madrid earthquake area landward of Mississippi levees during major high waters too. These sand boils are the effect of seepage pressure which is another independent cause of liquefaction of sand (Turnbull 1961).

Phenomenon of liquefaction to a bigger extent than that of New Madrid, occurred as the result of the Bihar-Nepal earthquake of 1934, India (Officers 1939). The area of so-called slump-belt, north of the Ganges River between Motihari and Purnea, was 12,200 sq. km. in area, (300 km in length, 50 km in largest breadth) and it was lying entirely in isoseismal IX and X after Rossi-Forrel-Mercali. Scattered areas were found within a region of 46,000 sq. km. forming part of isoseismal VIII. An area of 1600 sq. km. was devastated by sand emission, which deposited layers of sand up to a thickness of 60 cm. on the surface.

In the slump belt, which means the area where tilting of houses and subsidence of ground were more marked, fissuring and emission of sand and water reached their maximum development. In this belt, buildings and vehicles slumped bodily into the alluvium, railway embankments 2 m high sunk down level with the surrounding country, and the general tendency was for elevations and depressions (bottoms of lakes) to approach a common level, such as liquefied sand has. Slump is attributed to the area, which received predominantly vertical shocks.

Springs were flowing out of wells, holes and fissures, going through impermeable surface stratum, to appear in the form of geysers to a maximum height of 1.8 to 2.4m. They were in their thousands around the slump belt and created minature volcanic craters of sand with heights up to 7m. In an area of 10,000 sq. m. were found up to 34 sand vents and cones with an average diameter of 60cm. For greater discharge of water craterlike hollows were created, with inner walls sloping towards the centre and maximum diameter up to 8m. The deposited material varied from coarse sand to very fine silt in accordance with the heterogeneous nature of the alluvial strata from which it was derived. Springs began some minutes after the shock and they continued to flow for up to three hours, which in the opinion of the author is the time required for sedimentation and compaction of liquefied layer of sand, retarded by restricted outflow of water through springs.

In the space of several minutes, the Ganges River disappeared in some places, and the river bed remained dry. Suddenly the river appeared again, but this time it spouted up with considerable force from cracks and fissures in the sand; the level of the river rose and it spread from bank to bank. In the author's opinion the disappearance of the river could be attributed to the filling of new pores, created in the sand during dilatation preceding the compaction of sand. The compaction of sand and the subsequent subsidence of the ground could explain the rise of ground water level

throughout the North River after the earthquake.

Values of acceleration calculated for assumed simple harmonic motion ranged up to 3,270 mm/s^2 (0.3g). Hypothetic biggest acceleration in the epicentre was 5,000 mm/s^2 (0.5g). The period of vibrations was 1.5 to 2 sec, biggest amplitude 30.8 cm. The violence of shock is attributed to postulated fault zone in the rock-bottom.

The earthquake of 1923 in Kwanto, near Tokyo, Japan, serves as another example to demonstrate that greater depth of recent deposits is causing greater damage of wood frame houses (Kanai 1956). Brick buildings showed the opposite behaviour, nevertheless, the percentage of damaged brick buildings was for any depth greater than for wooden ones. The depth of deposits ranged up to 40m.

A more recent earthquake which may be cited is the Jaltipan (Mexico) earthquake of 1959, where foundation failures resulted from liquefaction of sandy silt layers, caused by acceleration, ranging between 0.07 and 0.2g. The sudden subsidence of the surface was of the order of about one metre. It has been stated that the liquefaction in the Valdivia region, in Chile in 1960, was on a much larger scale. (Marsal 1961).

Observation shows that effects of the identical acceleration of an earthquake are different. They depend on the type of soil, the height of ground water level and the depth of soil layer. When the dominant period of an earthquake approaches the period of a structure, resonance effects are felt and damage to the structure is higher. Smaller acceleration could disturb the equilibrium of soil, achieved through bigger acceleration of another direction than the small one. Damage depends much on the direction of shock which can create eigher bending or bending with torsion in the building.

Due to many variables involved, it is necessary to study the behaviour of saturated sand by tests simulating vibrations occurring during earthquakes. This was done e.g. by K. Kanai (1956) and N.N. Maslov (1957); and T. Mogami (1953) who experimented with related problems of dry sand.

The author attempted to solve the behaviour of saturated sand during vibration by the use of dimensional analysis, which disclosed that it is necessary to take into account simultaneously acceleration, frequency, height and volume of saturated sand. The result of the analysis was checked with experiments in the Laboratory of Foundation Engineering of the Civil Engineering Department, Technical University, Prague.

The author has tested vibration liquefaction only. There exists a similar problem of thixotropic liquefaction in the sand containing greater percentage of clay fraction or thixotropic liquefaction in saturated loess or clay with thixotropic properties (Mitchel 1960). In the author's opinion the earthquake in Kansu, China, in 1920, could be regarded as thixotropic liquefaction. The earthquake in Kansu was followed by landslides of loess to a colossal extent. Shortly before the earthquake torrential rains saturated several metres of surface layer of loess deposits, which

were normally dry. Their thickness was several hundreds metres. As a result, when the structure of saturated surface layer of loess was destroyed by the shock, it slid down some slopes for a distance of up to five kilometres. The soil bore the appearance of having shaken loose, clod from clod, and grain from grain, and then cascaded like water, apparently being thixotropically liquefied by the shock of the earthquake (Schultz, Cleaves 1955). Thixotropic softening of clay is also observed under the repeated applications of load to clay formations beneath railway tracks (King 1957). Expression of clay behaviour during vibration through thixotrophy is promising to give better explanation than expression through sensitivity of clay, normally used.

EFFECTS OF WAVE PROPAGATION ON THE STABILITY OF SATURATED SAND

Saturated sand is composed of grains, which are lying loose one upon another and the pores between grains are completely filled with water. Vibration caused by earthquake propagates from the bottom of the layer, from underlying to overlying grains, and also through the water. In the whole sand mass it develops forced wave propagation, which was studied by the author elsewhere (Bazant 1964).

Let us consider the vertical vibration of base. The first layer of sand grains, lying directly on base, is raised up firstly, while the overlying grains do not move, and compression of sand results. Successively, all the layers are in motion. Then the base begins to fall and the first layer of sand follows. Up to this time the overlying layers are rising and, therefore, dilatation of the sand developes. Forced wave propagation creates alternating compression and dilatation in the sand, which causes for small acceleration a small compaction of sand. Greater acceleration results in the liquefaction of sand, which is a transitory state followed by a great compaction.

Wave propagation has longitudinal, transversal and torsional components but we consider only longitudinal and vertical components. If the longitudinal wave propagation is accompanied by transversal and torsional wave propagation, the movement of grains and the compaction are facilitated.

Dissipation of wave energy is neglected, because the energy of an earthquake is supposed to be sufficient for unrestricted wave propagation through the whole depth of the layer. The fact than an earthquake creates time-limited vibration or a series of impacts followed by damped vibration, is neglected too. Owing to these neglected phenomena, our results are more conservative than is actually the case.

Let us now consider the effect of state of stress in soil for constant acceleration with the aid of methods used in soil mechanics (Terzaghi 1943). Generally, there exists a triaxial state of stress. As a simplification we will consider one-dimensional stress only. Wave propagation adds to the static stress by pulsating dynamic stresses in grains and water. The effective dynamic normal stress in saturated soil is given by

$$\sigma'_d = \sigma_s + \sigma_d - u_s - u_d \qquad (1)$$

where σ is the normal stress due to weight of soil and surcharge on surface, u pore pressure, subscript s denotes static value and d dynamic value. From Mohr envelope S for static case (Fig.1) we obtain shear stress

$$\tau_s = \sigma_s' \tan \phi \tag{2}$$

where

$$\sigma_s' = \sigma_s - u_s \tag{3}$$

denotes static effective stress and ϕ angle of internal friction.

At the beginning of a vibration, before compaction has altered the density, it is possible to assume $\phi_d = \phi_s = \phi$. Then dynamic shear stress is

$$\tau_d = \sigma_d' \tan \phi \tag{4}$$

and corresponding Mohr envelope D for dynamic case, supposed to be valid for constant acceleration, is given in Fig. 1. Similar envelope for changing acceleration was given by G. Tournon (L'Hermite 1948).

We assume that for rising acceleration α Mohr's envelope changes. For small α envelope D is identical with S. For greater α envelope D has the shape given by Fig. 1.

From envelope D it follows for small effective stress $\sigma_s' < \sigma_1'$ that $\tau_d \to 0$. Then after eq. (4), because $\phi \neq 0$, dynamic effective stress is

$$\sigma_d' = 0 \tag{5}$$

which indicates, that the strength of soil is zero. In consequence, saturated sand behaves like a liquid and this phenomenon is called vibration liquefaction of sand. During vibration liquefaction the effective dynamic stress after eq. (1) and (3) is

$$\sigma_s' + \sigma_d - u_d = 0$$

from which it follows

$$\sigma_s' = -(\sigma_d - u_d) \tag{6}$$

Eq. (6) shows, that in the case of vibration liquefaction the dynamic pore pressure u_d diminished by dynamic total stress σ_d equals static effective stress σ_s'. The negative right side of eq. (6) we denote

$$-\sigma_p = \sigma_d - u_d \tag{7}$$

Then σ_p is the expansion pressure of saturated sand created by wave propagation, and the pressure of sand on the casing of the container resembles behaviour of expanding gas.

For greater effective stress σ_s', governed by the condition $\sigma_1' < \sigma_s' < \sigma_2'$ dynamic tangential stress is $\tau_d < \tau_s$. Inserting eq. (3) and (7) in eq.

(1), the corresponding dynamic effective stress is the static effective stress diminished by expansion pressure

$$\sigma_d' = \sigma_s' - \sigma_p \tag{8}$$

Static strength of saturated sand is diminished by wave propagation, dilatation of sand occurs and compaction follows. Maximal expansion σ_p pressure, and therefore maximal compaction is reached after Fig. 1 for $\sigma_s' = \sigma_2'$, where σ_2' corresponds to the point of tangency of the tangent to envelope D, holding angle Φ from horizontal.

If σ_s' rises above σ_2', e.g. when the observed point lies in greater depth or when heavy building is founded on the surface of sand, the sand is compressed more effectively than for lower σ_s', expansion pressure σ_p is smaller (see Fig. 1.) and compaction is also smaller.

When, instead of expansion pressure σ_p, we are interested in pore pressure u only, we can measure in a piezometric tube hydrodynamic pressure u_d, which is the excess over known hydrostatic pressure u_s. This was done by N.N. Maslov (1957). Hydrodynamic pressure is caused by resistance of water against upward and downward motion of grains. Pore pressure for triaxial state of stress was studied by Huang Weng - Xi (1961).

DYNAMIC STABILITY AND CRITICAL ACCELERATION

Dense sand cannot be compacted by vibration during the earthquake, because its dilatation is so small, that not a single grain can move. We denote this sand as having dynamic stability. For a given unit weight of sand, which can be appropriately expressed by dry density γ_d, it is possible to determine critical acceleration α_c, which is the criterion of dynamic stability. The respective density is called vibration density γ_{dv}.

Dynamic stability is preserved, if dynamic effective stress - given by eq. (8) - is only a little smaller than the static one, which could be represented in Fig. 1. by the curve D approaching envelope S. This is fulfilled for

$$\sigma_p \to 0 \tag{9}$$

from which after eq. (7) it follows approximately

$$u_d = \sigma_d \tag{10}$$

Eq. (10) is possible for dynamic pore pressure $u_d \to 0$ only.

For accelerations smaller than critical $\alpha < \alpha_c$, the wave propagation creates only elastic movements in sand and any footing resting on sand undergoes no vibration settlement. This condition is necessary to be achieved for foundations of vibrating machines, especially for steam turbines coupled to a generator.

Let us assume that critical acceleration α_c is the function of dynamic effective stress, defined by eq. (8), as static effective stress diminished by expansion pressure.

As it was shown (Bazant 1964), static effective stress is the function

$$\sigma_s' = f(\gamma_{dv}, \gamma_w, H) \tag{11}$$

where γ_{dv} is vibration density, γ_w unit weight of water, H height of sand layer.

Expansion pressure is the function

$$\sigma_p = f(\gamma_{dv}, \gamma_w, A, g, V) \tag{12}$$

because it is the function of a one-dimensional wave propagation governed by wave equation

$$\frac{\partial^2 w}{\partial t^2} - v_p^2 \frac{\partial^2 w}{\partial z^2} = (\Phi_v - T) + mg \tag{13}$$

where w denotes vertical displacement, z vertical distance from origin, t time, v_p velocity of push wave, Φ_v external variable force, supposed as harmonic and acting with amplitude A on the volume of sand V, T resistance of water against displacements of grains, mg gravity force.

Taking into account variation of wave velocity with frequency f and considering natural frequency f_n for the case of resonance, we get in combination with eq. (11) and (12) the general form of critical acceleration (or compaction) function sought for

$$f(\gamma_{dv}, \gamma_w, f, f_n, A, g, H, V) = 0 \tag{14}$$

Applying dimensional analysis (Murphy 1952) we get from eq. (14) the dimensionless function of five variables only

$$f\left(\gamma_{dv}/\gamma_w \cdot f/f_n \cdot \alpha_c/g \cdot H^3/V \cdot A/H\right) = 0 \tag{15}$$

where γ_{dv}/γ_w denotes relative dry density, f/f_n relative frequency, α_c/g relative critical acceleration, H^3/V form factor, A/H relative amplitude. Critical acceleration α_c is here inserted as proportional to product $f^2 A$ obtained by dimensional analysis. The form factor represents the influence of triaxial state of stress in a container with rigid casing.

Assuming A/H to be negligible, we determine relative critical acceleration α_c/g from Fig. 2 as the function of $\gamma_{dv}/\gamma_w \cdot f/f_n$ and H^3/V. Because the dynamic behaviour of each sand may be very different, it is necessary to test the function for each sand and initial relative dry density γ_{dv}/γ_w separately.

The results, plotted on Fig. 2 in coordinates $\gamma_{dv}/\gamma_w \cdot \frac{\alpha_c}{g}$ as the

set of curves $f/f_n \cdot H^3/V$, were obtained in a glass container with a diameter of 96 mm, which was attached to a vibrating table moving vertically. The sand tested had grain size 0.2 to 0.5 mm, $\Phi = 35^o$, $\gamma_s = 2.674$ g/cm^3, $f_n = 37$ cps. Three initial densities were prepared, $n = 45\%$, $\gamma_d = 1.47$ g/cm^3, $n = 43\%$, $\gamma_d = 1.524$ g/cm^3 and $n = 41\%$, $\gamma_d = 1.578$ g/cm^3. Sand poured in water had a porosity of 46% and compaction to desired density was obtained by horizontally striking the glass container with a rubber hammer. Acceleration was measured electrically, as it was found, that assumption of sinusoidal vibration giving $\alpha = 4\pi^2 f^2 A$, was fulfilled for the vibration table used only in part of the range of studied amplitudes and frequencies.

From Fig. 2 it is possible to find relative critical acceleration α_c/g for each relative vibration dry density γ_{dv}/γ_w, knowing initial dry density. If relative density of sand in situ is for given α_c/g higher than required by Fig. 2, it can be stated that sand has dynamic stability. Therefore, the field measurement of profiles of sand density is one of crucial points of examination. The irregular shape of curves in Fig. 2 is inevitable, because for each combination of amplitude and frequency the values of neglected transversal and torsional wave propagation are changing.

Prediction of dynamic stability of saturated sand during earthquake is governed by model laws. Model laws require the same density, frequency and acceleration in model and prototype. Dimensions of layer of sand need to be geometrically similar. Neglected argument A/H should require geometric similarity of amplitudes, which is not possible to fulfill, because acceleration does not alter. According to model laws it is necessary to extend Fig. 2 by tests of frequencies around 1 cps and of form factor $H^3/V \to 0$.

The attainment of dynamic stability in nature according to result of tests given in Fig. 2 is possible, when vibration takes time, which is necessary for water to escape in all the pores of the sand layer through the longest seepage path. If there is a brief earthquake, dynamic stability for given acceleration is not attained.

From Fig. 2, Fig. 3 is derived showing for different accelerations α the decrease of compaction $\gamma_{dv} - \gamma_d$ for decreasing porosity n. Fig. 3 is for the purpose of finding the required compaction of sand which will assure dynamic stability. Suppose that criterion of stability requires $\gamma_{dv} - \gamma_d < 0.005$ g/cm^3, then for $H^3/V = 0.7$ after Fig. 3, stability can be achieved for $\alpha/g = 0.2$ sand with $n = 41\%$ only, ($\gamma_d = 1.578$ g/cm^3). Relative acceleration $\alpha/g = 0.3$ requires $n < 41\%$ and relative acceleration $\alpha/g = 0.4$ requires sand with still smaller porosity. Even smaller porosities will be required for $H^3/V < 0.7$, which shows that sand layers of greater area are more dangerous. The effect of decrease of frequency is not noticeable.

Proof of the validity of eq. (15) requires testing with containers of different diameter. Containers with diameter 96mm and 209mm were tested. Tests should give for both diameters and identical parameters the identical curves. Preliminary result shown on Fig. 4 for $H^3/V = 0.7$. It can be seen, that the solution given by eq. (15) is not perfect, probably due to

neglected triaxial state of stress. Nevertheless, for relative accelerations $\alpha/g < 0.2$ difference of relative dry densities is smaller than 0.02, which can be taken as acceptable.

Effect of surcharge on surface represented by the weight of building or weight of dynamically inert and porous soil, such as gravel, can be studied on models conserving model law requiring decrease of surcharge in proportion to decrease of geometric dimensions. It is not possible to assume that surcharge in model and in nature could be identical, as was sometimes done.

LIQUEFACTION AND LIQUEFACTIONAL ACCELERATION

Vibration liquefaction (for short liquefaction) encountered during earthquakes with acceleration which we assume to be greater than about 0.05 g, is the result of zero dynamic tangencial stress τ_d, and in consequence after eq. (5) of zero dynamic effective stress $\sigma_d' = 0$. From eq. (8) it follows as condition of liquefaction

$$\sigma_s' = \sigma_p \tag{16}$$

In other words, liquefaction is developed if for given dry density acceleration is reaching the value called liquefactional acceleration α_l, which causes expansion pressure $-\sigma_p = \sigma_d - u_d$ to annulate given static effective stress $\sigma_s' = \sigma_s - u_s$.

Let us assume that liquefactional acceleration α_l is the function of expanding pressure and static effective stress. Static effective stress is the function given by eq. (11) and expansion pressure by eq. (12). Then liquefaction is governed by the same function as dynamic stability and it is therefore also characterized by eq. (15).

There are four possible methods for measuring liquefaction. The first method is the penetration of metal bar in sand which should be total in first seconds of vibration if the whole height of layer is liquefied. The second method is the measurement of viscosity of liquefied sand with the aid of a sphere dipping into the soil. The third method is the measurement of hydrodynamic pore pressure, which for the case of liquefaction should give the pore pressure

$$u_d = \gamma' z \tag{17}$$

where γ' denotes unit weight of submerged soil and z depth of point of measurement beneath surface. It is possible to measure pore pressure at different depths by means of piezometer tubes attached to a glass container provided with a filter preventing sand from entering. The fourth method is measurement of dynamic shear stress which should be zero. It is necessary to find some new simple method enabling rapid measurement, because liquefaction in the container disappears in a few seconds.

The results of measurement of liquefaction obtained through the penetration method are plotted on Fig. 5 as the set of curves f/f_n and H^3/V in coordinates α/g and γ_d/γ_w. The sand used was the same as in tests

of Fig. 2. Accuracy of results is $\pm 0.05\ \alpha_l/g$. From Fig. 5 it is possible to find relative liquefactional acceleration α_l/g for relative vibration dry density up to $\gamma_{dv}/\gamma_w = 1.50$. E.g. for $\gamma_{dv}/\gamma_w = 1.47$ sand liquefies for liquefactional acceleration $\alpha_l/g = 0.55$, if $H^3/V = 0.7$ and $f/f_n = 0.54$. It was not possible to determine the liquefaction for frequencies smaller than 20 cps, because the vibration table was not producing the necessary acceleration. The penetration method failed also for densities higher than 1.5 g/cm^3, because only the upper part of sand layer was liquefied.

From Fig. 5 it can be derived that for increasing volume $H^3/V \to 0$ the danger of liquefaction increases and liquefaction occurs for smaller acceleration. This case is usually encountered in natural conditions.

In contrast if for the height H of saturated sand layer H^3/V is increasing, the danger of liquefaction decreases and liquefaction occurs for greater acceleration.

From Fig. 5 we would assume that decreasing the frequency will increase the danger of liquefaction.

The comparison of dynamic stability (Fig. 2) and liquefaction (Fig. 5) shows, that for higher γ_{dv}/γ_w liquefaction follows immediately after the loss of dynamic stability and both phenomena merge into a single one, even if it is supposed, in a theoretical way, that it should be $\alpha_l > \alpha_c$.

The condition $\sigma_s' = \sigma_p$ is fulfilled for smaller acceleration for the upper part of the sand layer only. In this case, the upper part of the sand layer is liquefied, but the lower part undergoes compaction only. The final subsidence of surface is smaller than for the layer, which liquefies over the full height, and collapse of the building is to be expected to a smaller extent than for liquefaction of the whole height of sand layer. It is also possible to determine a foundation depth at which the sand will not liquify.

COMPACTION

There are cases, which range between dynamic stability and liquefaction. Saturated sand is not stable, but neither is it liquefied, because expansion pressure σ_p does not equal static effective stress. This holds after Fig. 1 for static effective stress $\sigma_s' > \sigma_p$ and for accelerations, which we assume to be greater than about 0.02 g, depending on dry density of sand. Dynamic effective stress is given by eq. (8) and compaction of sand follows (Bazant 1964). Compaction is going on, until relative density given by Fig. 2 is reached. Subsidence of surface and irregular settlement of buildings follow the compaction. Therefore, in this case also damaged buildings have been observed during earthquake.

If the saturated sand is covered by a clay layer, the water squeezed from the sand during compaction (or liquefaction) finds its outlet in weak spots or holes through the clay. Sand carried by the water forms

small volcanoes on the surface. The phenomenon of squeezing water is delayed and takes longer than in the case where the clay layer is absent.

PREVENTIVE MEASURES

The earthquake damage of buildings on saturated sandy subsoil can be effectively reduced by compaction of layers of loose sand through which vibration density γ_{dv} holding for given parameters is achieved. For compactions of saturated sand vibroflotation can be used. A cheap method of compaction is blasting which can be used in newly developed areas, where no damage to underground utilities and nearby buildings can be caused. Foundations on piles, reaching to a depth where saturated sand does not liquefy, are another possibility.

BIBLIOGRAPHY

Bazant Z. (1964). Compaction of saturated sand by upward vertical vibration, Proc. of Seminar on Soil Mechanics, Warsaw, Poland. p. 601.

Fuller M. (1912). New Madrid Earthquake, Bull. of U.S. Geolog. Survey, Nr. 494., D.C.

Huang Wan-Xi (1961). Investigations on stability of saturated sand foundations and slopes against liquefaction, Proc. Fifth Int. Conf. Soil Mech. and Found. Eng. Paris, Dunod Vol. II, p. 629.

Kanai K., Takahasi R., Kavasumi H. (1956). Seismic characteristics of soil, Paper 31, Proc. World Conf. Earthquake Eng., Berkeley, Calif.

King K.H. (1957). Tests to determine the behaviour of rail-track formations on various soil subgrades with particular reference to clays, Proc. Fourth Conf. Soil Mech. and Found. Eng. London, Butterworths, Vol. II, p. 128.

L'Hermite R., Tournon G. (1948). La vibration de béton frais Annales de l'Inst. tech. du Bâtiment et de Travaux Publ., No. 11, Nouvelle serie, Paris.

Marsal R.J. (1961). Behaviour of a sandy uniform soil during the Jaltipan earthquake, Mexico, Proc. Fifth Conf. Soil Mech. and Found. Eng., Paris, Dunod, Vol. I, p. 229.

Maslov N.N. (1957). Questions of seismic stability of submerged sandy foundations and structures, Proc. Fourth Int. Conf. Soil Mech. and Found, Eng., London, Butterworths, Vol. 1, p. 368.

Mitchel J.K. (1961). Fundamental aspects of thixotropy in soils, Trans. Am. Soc. Civ. Eng., Vol. 126, Part I, p. 1586.

Mogami T., Kubo K. (1953). The behaviour of soil during vibrations, Proc. Third Int. Conf. Soil Mech. and Found. Eng., Zürich, ICOSOMEF, Vol.I, p.152.

Murphy G. (1952). Similitude in engineering, New York, Ronald Press.

Officers of the Geological Survey (1939). The Bihar-Nepal earthquake of 1934, Memoirs of the Geological Survey of India, Vol. 73, p. 32.

Schultz J.R., Cleaves A.B. (1955), Geology in engineering, New York, Wiley.

Terzaghi K., (1943). Theoretical soil mechanics, New York, Wiley.

Turnbull W.J., Mansur C.J. (1961). Design of control measures for dams and levees, Trans. Am. Soc. Civ. Engineers. Vol. 126, Part I, p. 1486.

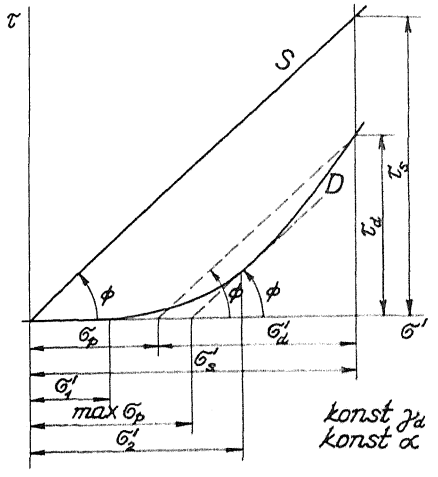

Fig. 1 Mohr's diagram of saturated vibrating sand

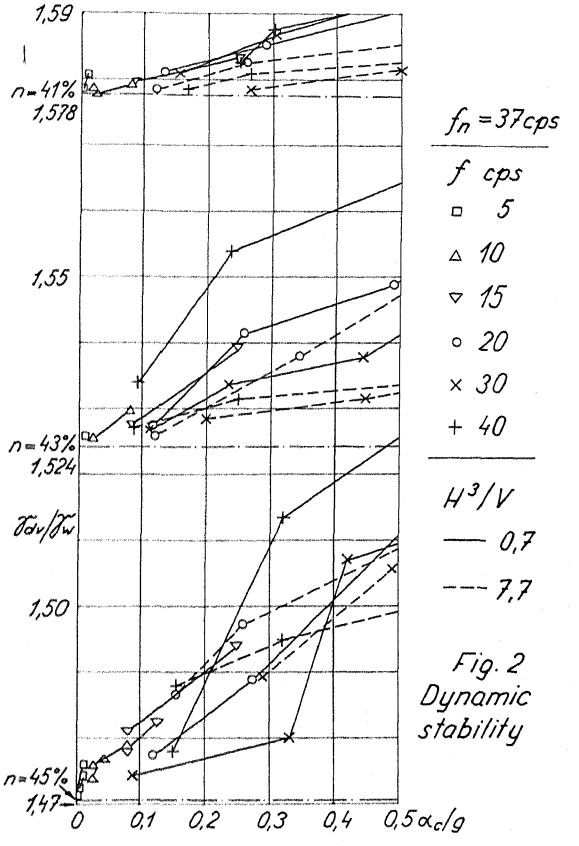

Fig. 2 Dynamic stability

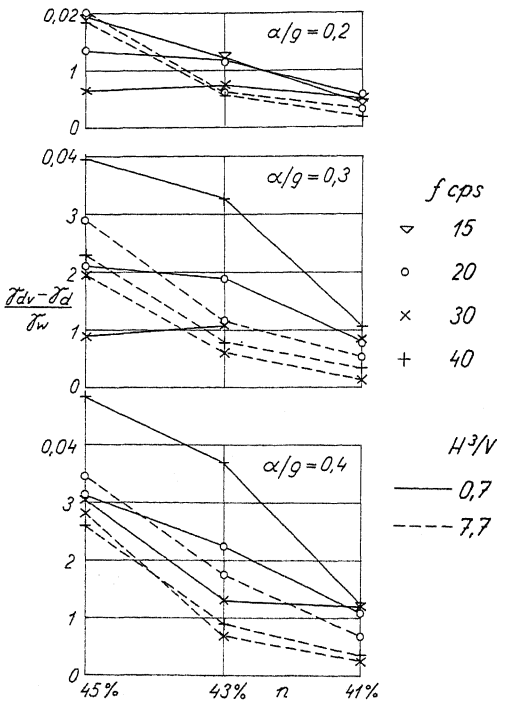

Fig. 3. Influence of porosity on the degree of compaction

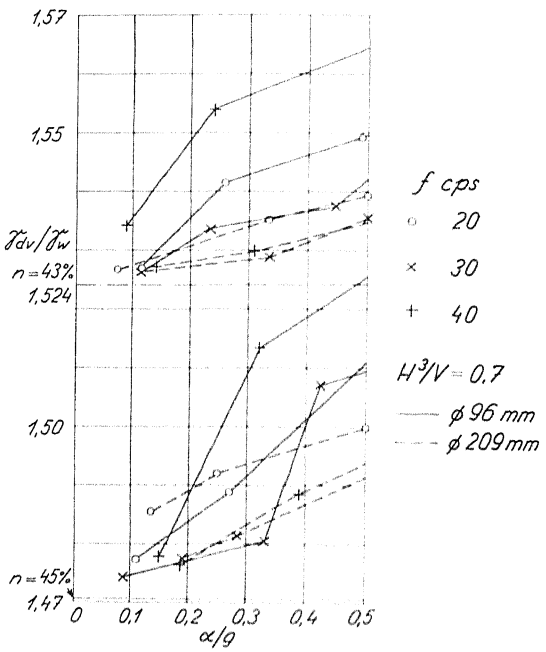

Fig. 4. Vibration density for different diameters.

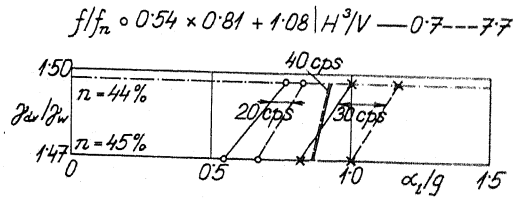

Fig. 5 Liquefactional acceleration

STABILITY OF SATURATED SAND DURING EARTHQUAKE

BY Z. BAZANT

QUESTION BY: RONALD F. SCOTT - U.S.A.

How are the author's calculations, for example, eqs. (14 or (15), or experiments dependent on the soil's grain size or permeability?

AUTHOR'S REPLY: My theory is to treat the dimensional analysis of the problem, which establishes eq. (15), serving as a basis for the correct evaluation and interpretation of tests. Using eq. (15) it is necessary to test each sand separately. The model laws require that this sand should have the same density in model and in prototype. This means that for each grain size or permeability new tests are needed which consider the influence of both these factors automatically. Graphs given in my article refer to the sand tested; only they have no general validity.